Location of Ni2+ ions in siliceous mordenite: A computational approach

ARTICLE *in* THE JOURNAL OF PHYSICAL CHEMISTRY · JUNE 1990

Impact Factor: 2.78 · DOI: 10.1021/j100376a023

4 AUTHORS, INCLUDING:

Robert A Jackson
Keele University
142 PUBLICATIONS **1,691** CITATIONS
SEE PROFILE

Richard Richard A Catlow
University College London
998 PUBLICATIONS **25,884** CITATIONS
SEE PROFILE

Reprinted from The Journal of Physical Chemistry, 1990, 94.

Location of Ni^{2+} Ions in Siliceous Mordenite: A Computational Approach

C. J. J. den Ouden,*,† R. A. Jackson,‡ C. R. A. Catlow,‡ and M. F. M. Post†

Koninklijke/Shell-Laboratorium Amsterdam, Shell Research B.V., Badhuisweg 3, 1031 CM Amsterdam, The Netherlands, and Department of Chemistry, University of Keele, Keele, Staffordshire, ST5 5BG, United Kingdom *(Received: March 23, 1989; In Final Form: January 20, 1990)*

Lattice energy minimization calculations are performed to study the location of Ni^{2+} ions in siliceous mordenite. It is found that Ni^{2+} does not occupy well-defined extra-framework sites but that its location seems to be related to the occurrence of specific Al–O–$(Si–O)_N$–Al sequences in the siliceous lattice. This study also provides a possible explanation for the limited Ni^{2+} ion exchange capacity in siliceous zeolites.

I. Introduction

Zeolites are widely used as components in heterogeneous catalysts in the oil and chemical processing industries.[1,2] Both the dimensions of the zeolite micropores and the zeolitic chemical composition are of importance in the catalytic conversion of hydrocarbons into useful products.

It is well-known that zeolites in the H-form act like solid acids, the acidity primarily depending on the aluminum content in the zeolite lattice,[3] and hence are used as acidic catalysts. However, given the ion-exchange properties of zeolites, one is able to modify and tune the catalytic performance by introducing different cations via ion-exchange procedures. In particular the introduction of transition-metal ions into the zeolite lattice seems, and has already been shown,[4] to be very interesting because these ions exhibit catalytic activity in homogeneous as well as heterogeneous catalysis. Therefore, ion-exchange studies are important both from a practical and from a fundamental point of view.

Several research groups[5,6] have investigated the exchange properties of monovalent and divalent metal ions in siliceous zeolites. Whereas monovalent ions reveal complete exchange ($M^+/Al = 1.0$), the ion-exchange properties for divalent metal ions are less clear-cut and in general an incomplete exchange is found, i.e., $M^{2+}/Al < 0.5$.

Recently it has been reported that the extent of exchange in zeolite ZSM-5 depends on the lattice aluminum content.[7] On increasing the aluminum content, the M^{2+}/Al ratio slowly reaches the complete exchange value of 0.5. These exchange features for divalent ions were explained by using a statistical model for the exchange process in siliceous ZSM-5.[7] In that study, it was envisaged that during an ion-exchange process there is a competition between the incoming divalent cations and the monovalent ions present in the zeolite which are to be exchanged. After reaching equilibrium, the model assumes that the divalent cation has removed two monovalent ions from an Al–O–Si–O–Al sequence in the zeolite framework and is "anchored" in the zeolite by such a sequence. Sequences with more than one silicon between the Al sites are assumed not be able to coordinate divalent cations and thus no monovalent ions are removed in this case.

The location of divalent cations inside zeolites is still a matter of extensive debate. With high-alumina zeolites, the concentration of divalent cations attainable is in general sufficiently high to allow determination of their location by standard XRD techniques,[8] but with siliceous zeolites levels of exchange are too low to allow investigation of the location of divalent cations by these methods. Therefore, we followed a computational approach in order to unravel the siting preferences of divalent metal ions. The system chosen in our studies is nickel-exchanged mordenite, which has applications as a catalyst in a range of chemical reactions other than those requiring carbenium ions as intermediates.[9]

In general, two types of localization can be distinguished. Firstly, the Ni^{2+} ions can occupy well-defined extra-framework sites[10] within the mordenite lattice. The preference of Ni^{2+} ions for occupation of these extra-framework sites can be thought of as stemming from favorable electrostatic interactions of the Ni^{2+} ions with the local framework structure around these sites. Secondly, it is possible that the location of Ni^{2+} ions is indeed related to the distribution and siting of aluminum,[11] as has already been suggested earlier.[7]

In this paper, we will investigate both the above-mentioned possibilities for the case of Ni^{2+} in siliceous mordenite.

II. Computational Methods

The methods used in this paper are lattice energy minimization and defect lattice energy minimization. Both techniques are briefly described in this section.

II.1. Lattice Energy Minimization. This technique enables structures corresponding to minimum lattice energies to be calculated. This may be carried out at two levels: either the atomic positions only are adjusted until the energy minimum is found (constant volume minimization) or, in addition, the unit cell parameters are adjusted to remove any remaining strains in the lattice (constant pressure minimization). In this work, constant-pressure calculations are performed.

An additional feature of this work is that in some of the calculations the energy minimization is carried out in two stages: first, the framework of the siliceous zeolite is relaxed to its minimum-energy confirmation and then kept fixed while the extra-framework cations are adjusted to further minimize the energy.

II.2. Defect Lattice Energy Minimization. This technique can be used to model defects in structures (e.g., vacancies and interstitial framework positions). In this work, it is used to study the incorporation of aluminum and extra-framework cations into the siliceous zeolite structure.

The technique is based on the division of the lattice into two regions: region I surrounding the defect, and region II effectively modeling the rest of the lattice at long distances from the defect.

† Shell Research B.V.
‡ University of Keele.

(1) Maxwell, I. E. *Catal. Today* **1987**, *1*(4), 385.
(2) Hoelderich, W. F. *Pure Appl. Chem.* **1986**, *58*(10), 1383.
(3) See e.g.: Neuber, M.; Dondur, V.; Karge, H. G.; Pacheco, L.; Ernst, S.; Weitkamp, J. *Proceedings of the International Symposium "Innovation in Zeolite Materials Science", Nieuwpoort, Belgium (1987)*; Elsevier: Amsterdam, 1988; p 461.
(4) Minachev, Kh.; Isakov, Ya. I. In *Zeolites Chemistry and Catalysis*; Rabo, J. A., Ed.; ACS Monograph 171; American Chemical Society: Washington, DC, 1976.
(5) Chu, P.; Dwyer, E. G. *ACS Symp. Ser.* **1983**, *218*, 59.
(6) Matthews, D. P.; Rees, L. V. C. *Chem. Age India* **1986**, *37*(5), 353.
(7) Den Ouden, C. J. J.; Wierlers, A. F. H.; Kuipers, H. P. C. E.; Vaarkamp, M.; Mackay, M.; Post, M. F. M. *Stud. Surf. Sci. Catal.* **1989**, *49*.
(8) (a) Maddox, P. J.; Spachursky, J.; Thomas, J. M. *Catal. Lett.* **1988**, *1*, 191. (b) Thomas, J. M.; Williams, C.; Rayment, T. *J. Chem. Soc., Faraday Trans. 1*, **1988**, *84*(9), 2915.
(9) See e.g.: Wendt, G.; Hagenau, K.; Dimitrova, R.; Popova, Z.; Dimitrov, Ch. *React. Kinet. Catal. Lett.* **1986**, *31*(2), 383.
(10) (a) Mortier, W. J. *Compilation of extra Framework Sites in Zeolites*; Butterworth: London, 1982. (b) Mortier, W. J.; Pluth, J. J.; Smith, J. V. *Natural Zeolites* **1978**, *53*.
(11) Derouane, E. G.; Fripiat, J. G. *Proc. 6th Int. Zeolite Conf. Reno, NV* **1983**, p 717.

0022-3654/90/2094-5286$02.50/0

TABLE I: Potential Parameters for Zeolite Frameworks[12,15]

shell model	q_{core}	q_{shell}	A	β	C
Si^{4+}	4	0			
Al^{3+}	3	0			
O^{2-}	0.86902	−2.86902			
Ni^{2+}	−1.344	3.344			
Si···O			1283.907	0.32052	10.66158
Al···O			1460.3	0.29912	0.0
O···O			22764.0	0.149	27.88
Ni···O			1582.5	0.2882	0.0

3-body potential for O–Si–O and O–Al–O: k = 2.09724 eV·rad^{-1}; θ_0 = 109.47°

harmonic core shell potential for O: k = 74.92 eV·Å^2

harmonic core shell potential for Ni: k = 93.7 eV·Å^2

In region I, the atoms are treated explicitly and interact via interatomic potentials (see section II.3). In region II, the lattice is treated as a dielectric continuum. Further details are given in ref 12.

II.3. Potentials. The basic form for the potential describing the interaction of a pair of ions is given by the equation

$$V(r_{ij}) = q_i q_j / r_{ij} + A_{ij} \exp(-r_{ij}/\beta_{ij}) - C_{ij}/r_{ij}^6 \qquad (1)$$

Here, i and j refer to the interacting ions and q_i and q_j to their charges, and A_{ij}, β_{ij}, and C_{ij} are short-range potential parameters. The Coulomb terms are calculated by using an Ewald summation.

In all potentials, formal charges have been used. Ionic polarizability is incorporated by using the shell model[13] in which an ion is represented by a core and a shell joined by a harmonic spring; the sum of core and shell charges is the formal charge.

Finally, in order to be able to simulate framework relaxation in zeolites, it is necessary to include an extra term in the potential to take account of the directionality of the bonding of oxygen ions with silicon or aluminum ions. This term, which is defined for each O–Si–O or O–Al–O bond, takes the form

$$V_{3\text{-body}} = (1/2)k(\theta-\theta_0)^2 \qquad (2)$$

In this equation, k is the bond force constant and θ_0 is the equilibrium bond angle.

In the calculations reported, all parameters were defined by using a parametrization of the above potential form to α-quartz. The parameters are presented in Table I.

III. Calculations Performed

For the mordenite structure, we used the data of Mortier, Pluth, and Smith.[14] The positions of the symmetric extra-framework sites are derived by using data of Mortier et al.[10] Information and relative coordinates of both the mordenite lattice and extra-framework sites, together with the nomenclature used in this paper, are given in Table II.

Relative stabilities of the all-silica and Ni–aluminosilicate mordenites (unit cell compositions $Si_{48}O_{96}$ and $NiSi_{46}Al_2O_{96}$, respectively) were calculated by using the perfect lattice energy minimization procedure as described in the preceding section. Calculations are performed at constant pressure using the shell model. Table I lists the charges and the potential parameters used in the calculations.

A second approach was followed by considering the presence of framework aluminum and extra-framework Ni^{2+} in the zeolite lattice as defects in an otherwise all-silica lattice. These defect calculations were also performed using the shell model.

IV. Results

IV.1. Structural Effects. Perfect lattice energy minimization calculations were performed on mordenite containing two aluminum ions and one Ni^{2+} ion as charge-compensating cation per unit cell (Si/Al = 23). In order to study structural effects only, the aluminum ions were not placed at specific mordenite framework sites, but the resulting negative charge was smeared out over all T-sites.

TABLE II: Information on the Mordenite Structure Used

space group: *CmCm* (No. 63)
lattice parameters:
a = 18.65 Å
b = 20.45 Å
c = 7.66 Å
$\alpha = \beta = \gamma = 90°$
lattice energy of relaxed all silica lattice:
−12392.9 kJ/mol SiO_2 (shell model)

Extra Framework Sites: Relative Coordinates

notation used in this paper	corresp sites acc. to ref 10	x	y	z	multiplicity i =
I.*i*	I	0.0000	0.5000	0.0000	1–4
II.*i*	IV	0.0000	0.1825	0.7500	1–4
III.*i*	VI	0.1606	0.0000	0.7906	1–16
IV.*i*	VIII	0.0000	0.0000	0.0000	1–4

A Ni^{2+} ion was initially placed at the extra-framework sites I.1, II.1, III.1, and IV.1. The Ni^{2+} ion was allowed to relax to its minimum-energy position while the mordenite lattice was kept fixed at its minimum-energy configuration, which followed from an energy minimization on the all-silica structure (see Table II). The results of these four calculations are presented in Table III.

From Table III it can be seen that the Ni^{2+} ion has to be moved over a considerable distance before reaching a minimum. Starting from the four extra-framework sites, four different positions for the minimum are found corresponding to four different energies. This, as a matter of fact, indicates that the global energy minimum has not been found. However, Table III shows that the relative lattice energies for the four final Ni^{2+} positions are all very similar; thus it can be envisaged that the potential energy surface is very flat, which makes it likely that there is no preferential location of Ni^{2+} at extra-framework sites.

IV.2. Al–O–(Si–O)$_N$–Al Sequence Effects. Perfect Lattice Energy Minimization. As became obvious in section IV.1, no convincing evidence for siting of Ni^{2+} cations at specific ion-exchange sites in the mordenite framework emerged from our calculations. In this section, we concentrate on various Al–O–(Si–O)$_N$–Al sequences occurring in the zeolite framework ($N > 0$ to obey Lowenstein's rule). As will be shown, siting of Ni^{2+} ions can be directly related to the presence of specific Al–O–(Si–O)$_N$–Al sequences.

In general, three different environments for Ni^{2+} ions can be defined in the mordenite framework: the 12-ring main channel, the 8-ring channel (secondary pore), and the 8-ring side pockets of the main channels.

Ni^{2+} ions were placed in each of these locations in turn, combined with a specific Al–O–(Si–O)$_N$–Al sequence in the zeolite framework. The particular choice of locating the Al atoms at specific T sites in the three types of environment mentioned above is somewhat arbitrary, but it is assumed that the specific location of pairs of Al in a given environment will have only a secondary effect. The Ni^{2+} ion was allowed to relax to its minimum-energy position, while the zeolite lattice was kept fixed at its minimum-energy configuration (see Table II). In these calculations the Al–Al interaction is also taken into account.

Table IV represents the results obtained for Ni^{2+} ions in the three different locations combined with several Al–O–(Si–O)$_N$–Al sequences.

Ni^{2+} in the 12-Ring (Main Channel). The first section of Table IV displays relative lattice energies for Ni^{2+} located in the 12-ring main channel in combination with several sequences (N = 1–4) in the ring. Energies are calculated per mole of TO_2 (T = tetrahedral lattice site occupied by either Si or Al) or per 1/48 mol of $NiSi_{46}Al_2O_{96}$ and are given relative to the lattice energy and per mole of SiO_2 of the relaxed all-silica mordenite framework.

(12) Catlow, C. R. A. *Annu. Rev. Mater. Sci.* **1986**, *16*, 517.
(13) Dick, B. G.; Overhauser, A. W. Theory of the Dielectric Constants of Alkali Halide Crystals *Phys. Rev.* **1958**, *112*, 90.
(14) Mortier, W.; Pluth, J. J.; Smith, J. V. *Mater. Res. Bull.* **1975**, *10*, 1037.
(15) Lewis, J. V.; Catlow, C. R. A. *J. Phys. C.* **1985**, *10*, 1149.

TABLE III: Shell Model Calculations on Mordenite Containing One Ni^{2+} Ion/Unit Cell: $NiT_{48}O_{96}$

charge smeared out over T-sites: $q_T = 3.9583$
lattice energy for the all-silica structure: −12392.9 kJ/mol

initial Ni positn[a]			initial rel lattice energy,[b] kJ/mol TO_2	final Ni positn[a]			final rel lattice energy,[b] kJ/mol TO_2
z	*y*	*z*		*x*	*y*	*z*	
0.0000	0.5000	0.0000	180.6	−0.0054	0.5786	−0.2356	180.3
0.0000	0.1825	0.7500	202.3	0.4954	0.0777	0.6538	180.3
0.1606	0.0000	0.7906	181.9	0.1363	−0.0064	0.9317	181.4
0.0000	0.0000	0.0000	182.2	−0.0054	0.1779	0.2784	180.6

[a] Relative to a = 18.65 Å, b = 20.45 Å, c = 7.66 Å. [b] Relative to the lattice energy of the all-silica structure.

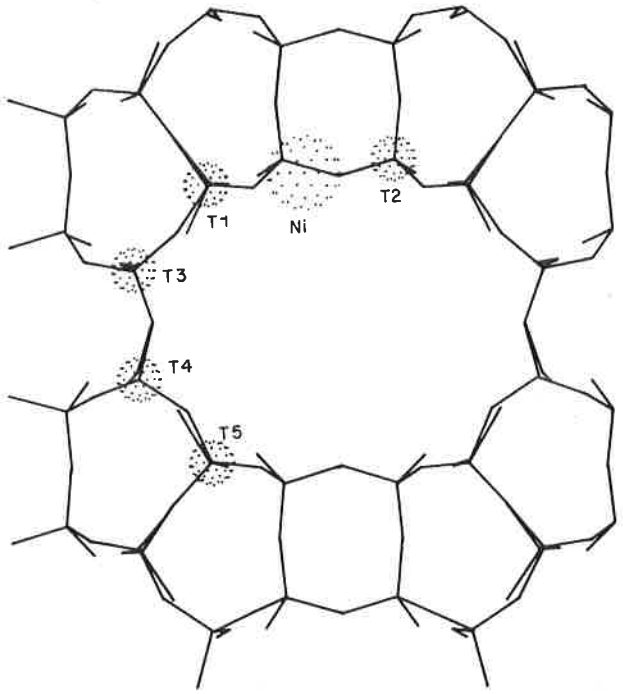

Figure 1. Positions of the aluminum atoms which form the various Al–O–$(Si–O)_N$–Al sequences in the 12-ring main channel. N = 1, T1–T2; N = 2, T2–T3; N = 3, T2–T4; N = 4, T2–T5. The Ni^{2+} position corresponds with the N = 1 sequence.

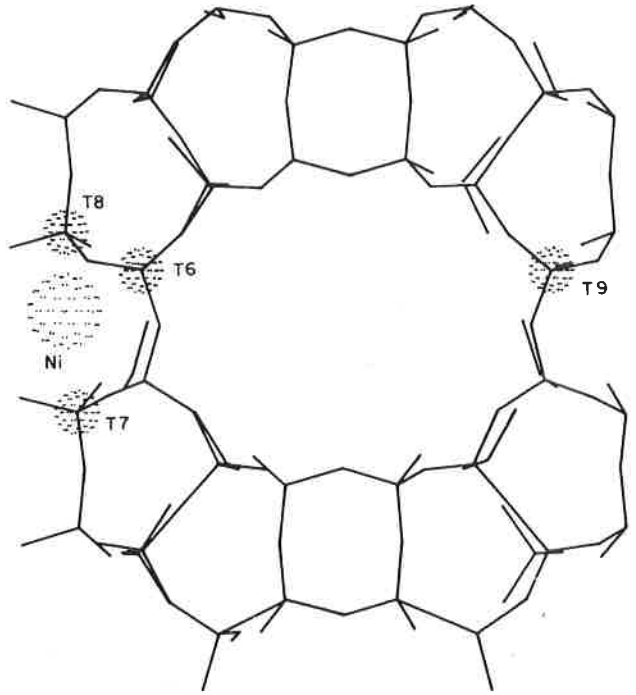

Figure 2. Positions of the aluminum atoms which form the various Al–O–$(Si–O)_N$–Al sequences in the 8-ring channel (secondary pore). N = 1, T6–T7; N = 2, T7–T8; N = 3, T7–T9. The Ni^{2+} position corresponds with the N = 1 sequence.

Figure 1 displays the aluminum positions chosen to obtain the various sequences.

It is obvious that Ni^{2+} is most strongly coordinated to the mordenite lattice when it is in the neighborhood of a sequence with N = 1. The energy gap observed when going from N = 1 to N = 2 is striking: Δ = 5.0 kJ/mol. This energy gap is much less pronounced when going from N = 2 to N = 3: Δ = 1.5 kJ/mol. An interesting feature appears for $N > 3$. Apart from a large energy gap between the sequences with N = 3 and N = 4, it can be seen that sequences with $N > 3$ are not able to coordinate Ni^{2+} ions to the mordenite lattice (no energy minima could be found).

In conclusion, one can say that Ni^{2+} located in the 12-ring main channel of mordenite is preferentially coordinated to an Al–O–Si–O–Al sequence (the aluminum atoms being labeled 1 and 2 in Figure 1) in the 12-ring. The corresponding position of the Ni^{2+} ion is also displayed in Figure 1. Furthermore, Al–O–$(Si–O)_N$–Al sequences with $N > 3$ are not able to coordinate Ni^{2+} to the mordenite lattice.

Ni^{2+} in the 8-Ring (Secondary Pore). The calculated results for Ni^{2+} located in the 8-ring are given in the second section of Table IV. The aluminum positions chosen to obtain the sequences are displayed in Figure 2. From the second section of Table IV, it is clearly seen that the energy gaps between the different sequences in the 8-ring are much less pronounced. Again, the sequence with N = 1 provides the strongest coordination of Ni^{2+} to the mordenite framework. It should be noted, however, that coordination of Ni^{2+} in the 8-ring is favored over coordination in the 12-ring by an amount of 0.3 kJ/mol. Furthermore, coordination of Ni^{2+} to a sequence with N = 2 in the 8-ring is only 0.1 kJ/mol less favorable than coordination to a sequence with N = 1 in the 12-ring. The position of the Ni^{2+} ion corresponding to the 8-ring Al–O–Si–O–Al sequence (the aluminum atoms for this sequence are labeled 6 and 7) is displayed in Figure 2.

Summarizing these results, we may conclude that Ni^{2+} is more strongly coordinated to the mordenite lattice in the 8-ring than in the 12-ring. The differences between several Al–O–$(Si–O)_N$–Al sequences are less pronounced, which might be due to the fact that the Al–Al distances in the various sequences in the 8-ring are relatively small compared to the Al–Al distances which are found in the 12-ring (see also Table IV).

Ni^{2+} in the 8-Ring Side Pocket. Results for Ni^{2+} located in the 8-ring side pocket are represented in the third section of Table IV. The positions for the aluminum atoms in the various sequences are displayed in Figure 3. Location of Ni^{2+} in a side pocket combined with an N = 1 sequence (aluminum atoms labeled 2 and T10) turns out to be the most stable configuration of all the calculations reported in this paper. The corresponding Ni^{2+} position is represented in Figure 3. Increasing N in the sequences very rapidly leads to unfavorable configurations.

IV.3. Al–O–$(Si–O)_N$–Al Sequence Effects. Defect Lattice Energy Minimization. Because of the similarities between the results obtained by the calculations described in section IV.2 and the defect lattice calculations, we will not discuss the results in detail. It suffices to note that both the perfect lattice and the defect calculations are in full agreement with each other. Apart from minor differences in the relative energies of the two types of computational approach, the trend of coordination of Ni^{2+} ions

TABLE IV: Shell Model Calculations on Mordenite Containing One Ni^{2+} Ion/Unit Cell: Ni Al_2Si_{46}[a]

N	Al on T site	position of framework Al x/a	y/b	z/c	Al–Al dist	equilib position of Ni^{2+} x/a	y/b	z/c	rel lattice energy,[b] kJ/mol of TO_2	
		1. Al–O–(Si–O)$_N$–Al Sequences in the 12-Membered Ring (Main Channel) (Figure 1)								
1	T1	0.2967	0.6910	0.5883						
					5.63	0.4461	0.6928	0.6880	137.8	
	T2	0.5821	0.7214	0.2915						Δ = 5.0
2	T3	0.1886	0.5788	0.4991						
					7.80	0.5116	0.6628	0.5725	142.8	
	T2	0.5821	0.7214	0.2915						Δ = 1.5
3	T4	0.1840	0.4304	0.5862						
					9.52	0.5161	0.6540	0.5606	144.3	
	T2	0.5821	0.7214	0.2915						Δ = 7.4
4	T5	0.2953	0.3143	0.4964						
					9.81	no minimum found			ca. 151.7	
	T_2	0.5821	0.7214	0.2915						
		2. Al–O–(Si–O)$_N$–Al Sequences in the 8-Membered Ring (Secondary Channel) (Figure 2)								
1	T6	0.1886	0.5788	0.4991						
					4.73	0.0716	0.5099	0.3818	137.5	Δ = 0.4
	T7	0.0753	0.3816	0.2911						
2	T8	0.0785	0.6236	0.7934						
					6.14	0.0311	0.5078	0.5621	137.9	Δ = 1.0
	T7	0.0753	0.3816	0.2911						
3	T9	0.9106	0.6233	0.7934						
					7.80	0.0216	0.5203	0.5681	138.9	
	T7	0.0753	0.3816	0.2911						
		3. Al–O–(Si–O)$_N$–Al Sequence in the 8-Membered Ring (Side Pocket) (Figure 3)								
1	T10	0.6907	0.6901	0.9988						
					5.67	0.5556	0.6995	0.0260	136.7	Δ = 3.3
	T2	0.5821	0.7214	0.2915						
2	T11	0.2953	0.6951	0.9992						
					7.40	0.5033	0.6850	0.6114	140.0	Δ = 1.7
	T2	0.5821	0.7214	0.2915						
3	T11	0.2953	0.6951	0.9992						
					7.75	0.4373	0.6831	0.8705	141.7	
	T12	0.6907	0.6901	0.5881						

[a] The lattice is fixed; the Ni^{2+} is allowed to relax. Relative lattice energy of the all-silica structure: −12392.9 kJ/mol of SiO_2. All lattice energies in this table are relative to the all-silica structure. [b] Relative to the lattice energy of the all SiO_2 structure.

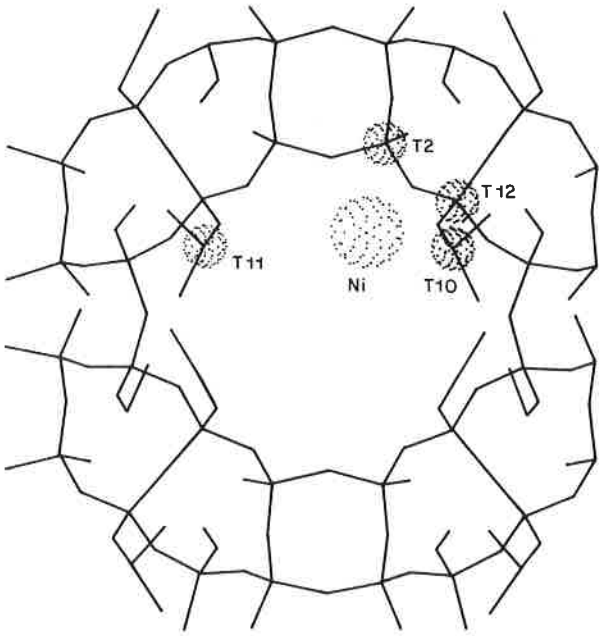

Figure 3. Positions of the aluminum atoms which form the various Al–O–(Si–O)$_4$–Al sequences in the 8-ring side pocket. N = 1, T2–T10; N = 2, T2–T11; N = 3, T11–T12. The Ni^{2+} position corresponds with the N = 1 sequence.

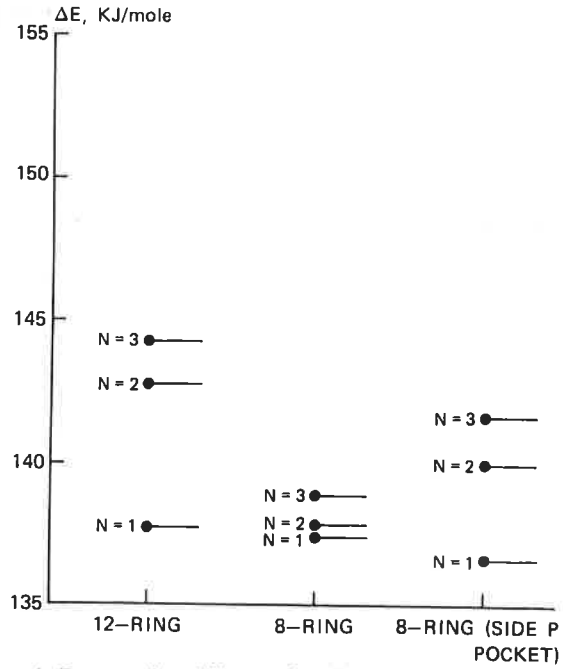

Figure 4. Framework stability as a function of the location of the Ni^{2+} ion and framework Al–O–(Si–O)$_N$–Al sequence. ΔE is the difference between the all-silica zeolite lattice energy and the Ni–aluminosilicate lattice energy. Decreasing ΔE means increasing Ni^{2+} localization preference.

to an Al–O–Si–O–Al sequence as the most stable one is fully reproduced in the defect calculations.

Furthermore, equilibrium positions for Ni^{2+} in combination with a particular sequence in the mordenite framework match up very well with the equilibrium positions found by using the perfect lattice approach.

V. Conclusions

In this paper, we have shown that, according to our calculations, the existence of specific extra-framework sites for Ni^{2+} in siliceous mordenite is doubtful. This conclusion is based on two obser-

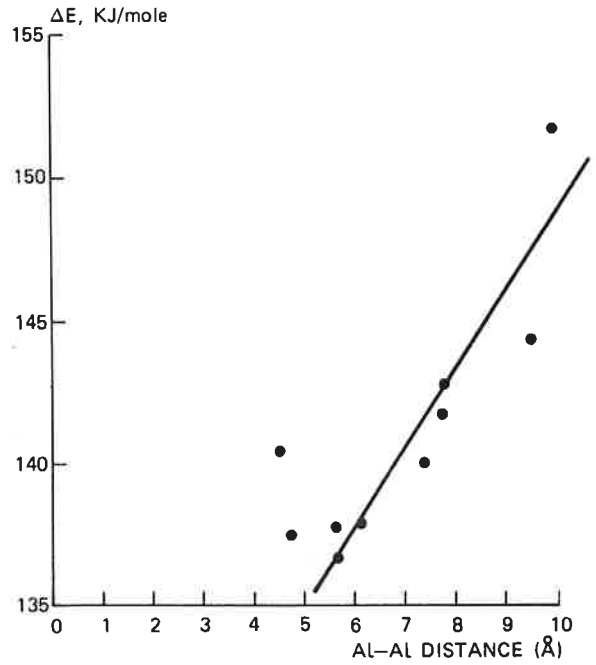

Figure 5. Framework stability as a function of Al–Al distance related to the location of Ni^{2+} ions in Ni–Aluminosilicate mordenite. Decreasing ΔE means increasing Ni^{2+} localization preference. The line is drawn as guide for the eye.

vations. Firstly, the small differences in the relative lattice energies for Ni^{2+} located at the four different extra-framework sites indicate hardly any preferences on structural grounds. Secondly, the relative lattice energies of the Ni–alumina mordenites are observed to depend on the existence of specific Al–O–(Si–O)$_N$–Al sequences in combination with a Ni^{2+} ion in close proximity (compare relative lattice energies in Tables III and IV). In particular, sequences with $N = 1$ turned out to be very stable in comparison to sequences with $N > 1$.

Not only the value of N but also the specific location of the Al–O–Si–O–Al sequences in the mordenite structure proves to be important. In this case ($N = 1$), our calculations clearly show that Ni^{2+} is preferentially located in the 8-ring side pocket, followed by location in the 8-ring secondary pore system. Location of Ni^{2+} in the 12-ring main channel proves to be less favorable. These findings are illustrated in Figure 4.

It should be noted that the choice of particular Al–O–(Si–O)$_N$–Al sequences studied in this paper is quite arbitrary. However, apart from N values for the various zeolite framework sequences, the Al–Al distances in the sequences also play an important role, allowing us to regard the sequences chosen as general representatives of sequences anywhere in the lattice. In particular in the case of Ni^{2+} located in the mordenite 8-ring secondary channel this Al–Al distance effect is clear. The fairly high stability of Ni^{2+} ions coordinated to Al–O–(Si–O)$_N$–Al sequences ($N = 2, 3$) in the mordenite 8-ring channel with respect to coordination to similar sequences in the 12-ring main pore system or the 8-ring side pocket is obviously (partly) related to Al–Al distances, as displayed in Figure 5.

At this point, it is worth noting that two Al framework atoms in close proximity to each other will result in an Al–Al repulsion due to the introduction of negative charge on the framework. However, this repulsion seems to be negligible compared to the interaction of these two Al atoms with a Ni^{2+} ion. Figure 5 clearly visualizes this feature.

In spite of the qualitative character of the calculations described in this paper, we feel that our study strongly supports the conclusions made earlier regarding the exchange properties of Ni^{2+} in siliceous zeolites.[7] The necessary occurrence of Al–O–(Si–O)$_N$–Al (with $N \leq 3$) sequences in the zeolite lattice to anchor Ni^{2+} explains the limited degree of Ni^{2+} ion exchange in siliceous zeolites: for a random distribution of aluminum (which we feel is for siliceous zeolites justified[7]) throughout the framework, the statistical probability of finding the necessary sequences is very small and thus exchange capacity is limited.

Acknowledgment. We thank Dr. M. Leslie (SERC Laboratories, Daresbury, UK) for assistance with a number of computational problems experienced during this work.

Registry No. Ni, 7440-02-0.